Bioorganic Chemistry 111 (2021) 104911

Contents lists available at ScienceDirect

Bioorganic Chemistry

journal homepage: www.elsevier.com/locate/bioorg

Tuning NO release of organelle-targeted furoxan derivatives and their cytotoxicity against lung cancer cells

Federica Sodano [a], Elena Gazzano [b], Barbara Rolando [a], Elisabetta Marini [a], Loretta Lazzarato [a,*], Roberta Fruttero [a], Chiara Riganti [c], Alberto Gasco [a]

[a] Department of Drug Science and Technology, University of Torino, 10125 Torino, Italy
[b] Department of Life Sciences and Systems Biology, University of Torino, 10123 Torino, Italy
[c] Department of Oncology, University of Torino, 10126 Torino, Italy

ARTICLE INFO

Keywords:
NO-donors
Furoxans
Mitochondrial Targeting
Anticancer Activity
Lysosomal Targeting

ABSTRACT

We herein report a study on a set of hybrid compounds in which 3-R-substituted furoxan moieties (R = CH_3, $CONH_2$, CN, $SO_2C_6H_5$), endowed with varying NO-releasing capacities, are joined to a mitochondrial probe, rhodamine B. Each product has been investigated for its ability to release NO both in physiological solution, in the presence of cysteine, and in A549 lung adenocarcinoma cancer cells. The cytotoxicity of all the products against the aforementioned cancer cells has been assessed, including the structurally related compounds with no mitochondrial targeting, which were taken as a reference. In the case of the models bearing the $–CH_3$ and $–CONH_2$ groups at the 3-position on the furoxan, only the targeted models showed a significant cytotoxic activity, and only at the highest concentrations, in accordance with their weak NO-releasing properties. On the contrary, the presence of the strong electron-withdrawing groups, as –CN and $-SO_2C_6H_5$, at the 3-position gave rise to anticancer agents, likely because of the high NO-releasing and of their capability of inhibiting cellular proteins by covalent binding. In detail, the rhodamine hybrid containing the 3-$SO_2C_6H_5$ substituted furoxan moiety emerged as the most interesting product as it showed high cytotoxicity over the entire concentration range tested. This substructure was also linked to a phenothiazine scaffold that is able to accumulate in lysosomes. Nevertheless, mitochondrial targeting for these NO-donor furoxan substructures was found to be the most efficient.

1. Introduction

Furoxan (1,2,5-oxadiazole 2-oxide, Chart 1) is a heterocycle system whose complex chemistry has been discussed in several reviews [1–4]. There is currently great interest in furoxan derivatives due to their ability to release nitric oxide (NO) in physiological conditions under the action of thiol cofactors [5–7]. As NO-prodrugs, furoxans display a wide range of biological activities, including anticancer properties [8]. The conjugation of NO-donor furoxan moieties with appropriate native drugs has been used as a strategy to generate a variety of hybrid structures, which act against more than one target simultaneously [8–13]. The 3-phenylsulfonylfuroxan moiety, a potent NO-donor, has been frequently used in the design of hybrid anticancer structures. It has been combined with antibiotics, cytotoxic drugs, non-steroidal anti-inflammatory drugs, enzyme inhibitors, multi-drug resistance (MDR) reversal agents and active natural products [14–15].

The most important cellular functions are localised inside cell organelles, thus, cytotoxic agents with innate tropism for these sites have increased efficacy. Drugs frequently lack affinity for a specific organelle and diffuse randomly within cells. The design of hybrid compounds obtained by joining drugs with vectors that can accumulate into one specific site, with particular attention to mitochondrion and lysosome, is an interesting strategy for overcoming this problem [16–20].

Mitochondria are key organelles that play a main role in the regulation of the cell cycle. As they exert a variety of functions, including energy production, redox metabolism and apoptosis, mitochondria are considered important targets for cancer drugs [21–22]. The design of hybrid molecules in which cytotoxic agents are conjugated with

Abbreviations: MDR, multi-drug resistance; LCD, lysosomal-mediated cellular death; LMP, lysosomal membrane permeabilization; ROS, reactive oxygen species; FR, folate receptors; PBS, phosphate buffer saline; LDH, lactate dehydrogenase.

* Corresponding author.
E-mail address: loretta.lazzarato@unito.it (L. Lazzarato).

https://doi.org/10.1016/j.bioorg.2021.104911
Received 20 November 2020; Received in revised form 5 January 2021; Accepted 7 April 2021
Available online 20 April 2021

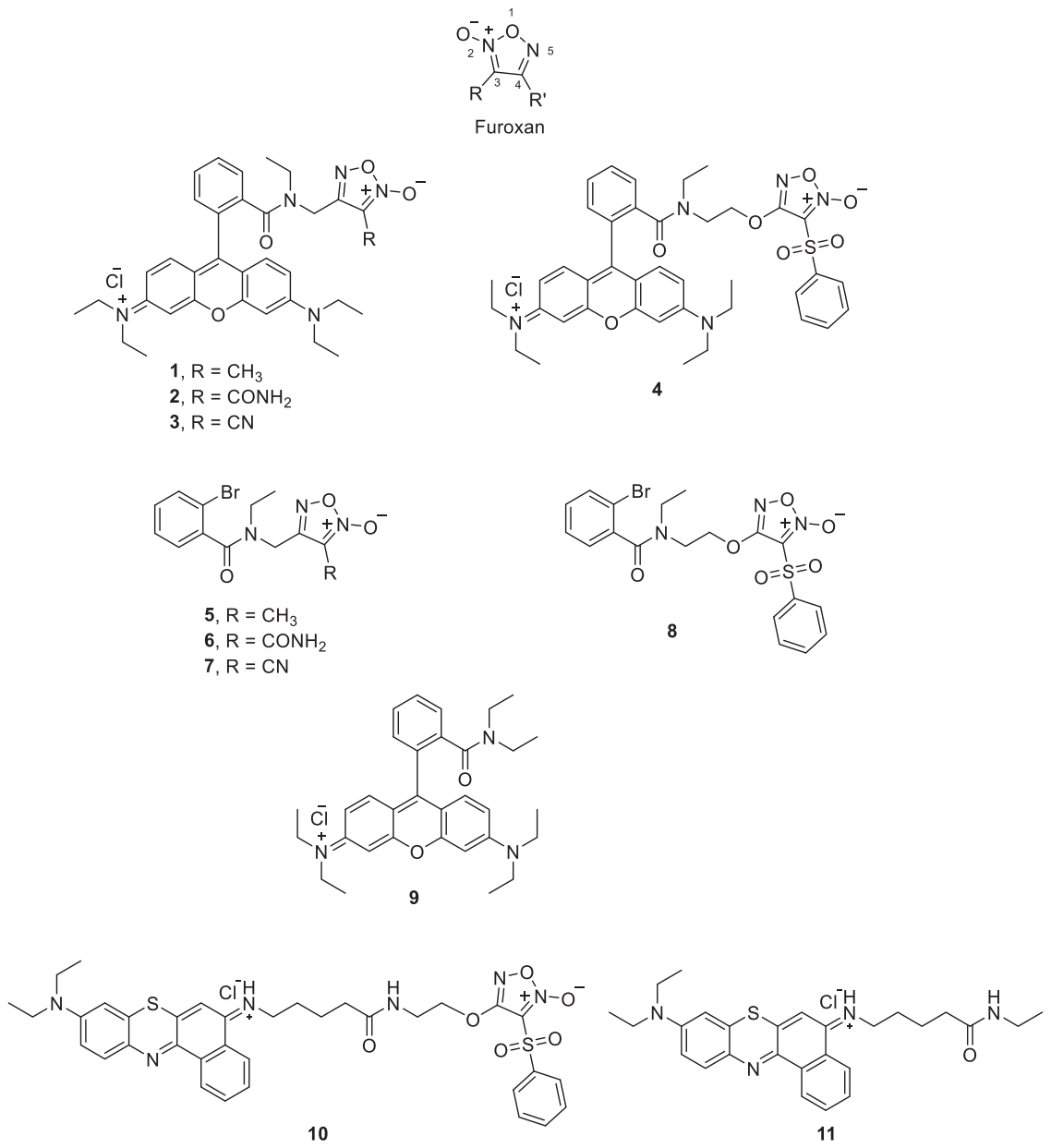

Chart 1. Chemical structure of hybrid and reference compounds.

mitochondrial-targeting lipophilic cations, such as triphenylphosphonium and rhodamine moieties, [23–25] represents a promising approach for the development of new antitumor drugs.

Lysosomes are acidic organelles (pH $\leq$ 5) and the site of hydrolytic enzymes, which are implicated in cellular digestion, immune responses, inflammasome activation, and drug resistance in cancer [26–27]. Also, they are involved in lysosomal-mediated cellular death (LCD), a process caused by lysosomal membrane permeabilisation (LMP) [26]. Depending on the degree of permeabilization, lysosomes can induce the release of enzymes in the cytosol, and thus give rise to apoptosis, autophagy and necrosis [26–28]. Cancer cells have large lysosomes that are endowed with a more fragile membrane than non-transformed cells, and are, therefore, more inclined to undergo LMP [28]. For these reasons, lysosomes are considered to be important targets for cancer therapy, [26,28–30] and the conjugation of agents that can provoke LCD to lipophilic vectors that display tropism for these loci has high interest.

NO is an important ubiquitous gaseous messenger, whose role depends on the dosage. At low concentrations (pM, nM), it displays protective and regulatory effects, while, at high concentrations (μM), it mediates toxicity [31,32]. NO exerts profound effects on mitochondria. Low NO concentrations modulate the mitochondrial electron transport chain and stimulate mitochondrial biogenesis. By contrast, high NO concentrations induce toxicity, principally via the inhibition of the tricarboxylic acid cycle and mitochondrial respiration [33]. NO is also involved in the regulation of lysosomal functions, although this aspect is still in need of thorough investigation. For this reason, there is great interest in NO tracking across lysosomes [34–35].

On this basis, we have designed a set of hybrid compounds **1**, **2**, **3** and **4** (Chart 1), in which furoxan substructures that are endowed with different NO-releasing capacities are joined to rhodamine B, a mitochondrial probe recently investigated by us [25]. The related non-mitochondrion-targeting furoxan derivatives **5**, **6**, **7**, **8** and the rhodamine derivative **9** (Chart 1) were synthesised as reference compounds. In the chemical structure of compounds **5**–**8**, the furoxan substructure was linked, through an appropriate bridge, to a phenyl substituted moiety bearing a bromine atom in the *o*-position. The bromine substituent is important to maintain a comparable lipophilic/hydrophilic balance with the rhodamine final derivatives.

The promising data regarding the mitochondrial targeting of the 3-phenylsulfonylfuroxan substructure has also driven us to link this moiety to a lysosomal probe. Compound **10**, in which the 3-phenylsulfonylfuroxan moiety was linked to a phenothiazine vector that displays lysosomal tropism, [35] and its reference compound **11**, were synthesised and evaluated (Chart 1).

The synthesis, lipophilicity and NO release of all compounds have been reported in this paper, togheter with the study of the reactivity of the furoxan ring towards thiol cofactors. The cytotoxicity of the hybrid molecules against A549 lung adenocarcinoma cancer cells had been compared with that of their reference compounds. Moreover, intracellular localisation in the same cell type was studied via confocal microscopy for compound **3**, and by fluorescence microscopy for compounds **4** and **10**.

2. Experimental section

2.1. Synthesis

All reactions involving air-sensitive reagents were performed under nitrogen in oven-dried glassware using the syringe-septum cap technique. All solvents were purified and degassed before use. Chromatographic separation was carried out under pressure on Merck silica gel 60 using flash-column techniques. Reactions were monitored using thin-layer chromatography (TLC) carried out on 0.25 mm silica-gel-coated aluminium plates (60 Merck F254) and using UV light (254 nm) as visualising agent. Unless otherwise specified, all reagents were used as received without further purification. Dichloromethane was dried over P_2O_5 and freshly distilled under nitrogen prior to use. DMF was stored over 3 Å molecular sieves. Anhydrous THF was freshly distilled under nitrogen from Na/benzophenone ketyl. Chemical shifts (δ) are given in parts per million (ppm) and the coupling constants (J) in Hertz (Hz). The following abbreviations were used to designate the multiplicities: s = singlet, d = doublet, t = triplet, q = quartet, m = multiplet, bs = broad singlet. ESI spectra were recorded on a Micromass Quattro API micro (Waters Corporation, Milford, MA, USA) mass spectrometer. Data were processed using a MassLynx System (Waters).

The purity of the final compounds was determined by RP-HPLC. Analyses were performed with a HP1100 chromatograph system (Agilent Technologies, Palo Alto, CA, USA) equipped with a quaternary pump (G1311A), a membrane degasser (G1379A), and a diode-array detector (DAD) (G1315B) integrated into the HP1100 system. Data analyses were processed using a HP ChemStation system (Agilent Technologies). The analytical column was a LiChrospher® 100 C18-e (250 × 4.6 mm, 5 μm) (Merck KGaA, 64,271 Darmstadt, Germany) eluted with CH_3CN 0.1% TFA/H_2O 0.1% TFA in a ratio that depended on the characteristics of the compound. All compounds were dissolved in the mobile phase at a concentration of about 0.01 mg/ml and injected through a 20 μL loop. HPLC retention times (t_R) were obtained at flow rates of either 1.0 or 1.2 mL/min and the column effluent was monitored using the DAD. The DAD acquired the UV spectra in the range from 190 to 800 nm, and the HPLC chromatogram was recorded at 226, 254, 580 and 660 nm (with 800 nm as the reference wavelength). The purity of the test samples was evaluated as the percentage ratio between the areas of the main peak and of possible impurities at the three wavelengths, and also using a DAD purity analysis of the chromatographic peak. The purity of all the target compounds was found to be ≥ 95%.

4-((Ethylamino)methyl)-3-methyl-1,2,5-oxadiazole 2-oxide (**14**). A solution of 4-(bromomethyl)-3-methyl-1,2,5-oxadiazole 2-oxide **12** (4.14 mmol, 800 mg)[36] in CH_3CN (10 mL) was stirred for 3 h at room temperature with an ethylamine solution 70 wt% in H_2O (20.7 mmol, 1.68 mL). After the reaction was complete, the mixture was extracted with DCM, washed with H_2O, brine and dried over anhydrous Na_2SO_4. The organic layer was concentrated to dryness to give target compound **14** (450 mg, 69%). ^{1}H NMR (600 MHz, $CDCl_3$) δ = 3.83 (s, 2H), 2.68 (q, J = 7.1 Hz, 2H), 2.18 (s, 3H), 1.28 (s, 1H), 1.10 (t, J = 7.1 Hz, 3H). ^{13}C NMR (150 MHz, $CDCl_3$) δ = 157.2, 113.0, 44.4, 43.8, 15.2, 7.9.

4-((2-Bromo-N-ethylbenzamido)methyl)-3-methyl-1,2,5-oxadiazole 2-oxide (**5**). A solution of 2-bromobenzoic acid **16** (1.35 mmol, 272 mg) in dry DCM (10 mL) was refluxed with $SOCl_2$ (4.05 mmol, 0.1 mL) for 12 h. The solvent was evaporated and the residue was taken up with toluene (30 mL), concentrated under reduced pressure three times in order to obtain **17** as a yellow oil. This intermediate was dissolved in dry DCM (10 mL), and compound **14** (1.35 mmol, 212 mg) and an excess of triethylamine (0.6 mL) were added, and the resulting solution was stirred for 3 h. The reaction mixture was washed with saturated sodium bicarbonate solution (2 × 15 mL), water (2 × 15 mL) and 1 M HCl (2 × 15 mL), then dried over anhydrous Na_2SO_4 and concentrated to dryness. Purification of the residue via silica gel chromatography, using DCM/Acetone (99/1, v/v) as the eluent, gave the target compound **5** as a white solid (300 mg, 65%). ^{1}H NMR (600 MHz, $CDCl_3$) δ = 7.57 (d, J = 8.1 Hz, 1H), 7.40 – 7.36 (m, 1H), 7.30 – 7.23 (m, 2H), 5.07 (d, J = 14.9 Hz, 1H), 4.54 (d, J = 14.9 Hz, 1H), 3.28 – 3.18 (m, 2H), 2.33 (s, 3H), 1.11 (t, J = 7.1 Hz, 3H). ^{13}C NMR (150 MHz, $CDCl_3$) δ = 169.5, 154.7, 137.3, 133.1, 130.8, 127.9, 127.7, 119.1, 113.2, 42.8, 37.8, 13.4, 8.3. ESI-MS $[M + H]^+$: *m/z* 340.3 and $[M + H + 2]^+$: *m/z* 342.3. HPLC purity ≥ 95% (CH_3CN 0.1% TFA/H_2O 0.1% TFA 70:30 (v/v), flow = 1.0 mL/min, t_R = 3.7 min), at 226 and 254 nm.

4-((2-(6-(Diethylamino)-3-(diethyliminio)–3H-xanthen-9-yl)-N-ethylbenzamido)methyl)-3-methyl-1,2,5-oxadiazole 2-oxide (**1**). A solution of N-(9-(2-(chlorocarbonyl)phenyl)-6-(diethylamino)–3H-xanthen-3-ylidene)-*N*-ethylethanaminium **18** (1.29 mmol, 642 mg) [25] in dry DCM (30 mL) was treated with compound **14** (1.29 mmol, 203 mg) and an excess of triethylamine (0.6 mL) and the resulting solution was stirred for 24 h. The reaction mixture was washed with saturated sodium bicarbonate solution (2 × 15 mL), water (2 × 15 mL) and 1 M HCl (2 × 15 mL), then dried over anhydrous Na_2SO_4 and concentrated to dryness. Purification of the residue via silica gel chromatography, using DCM/MeOH (90/10, v/v) as the eluent, gave target compound **1** as a mirrored purple solid (600 mg, 75%). ^{1}H NMR (600 MHz, $CDCl_3$) δ = 7.72 – 7.69 (m, 2H), 7.59 – 7.56 (m, 1H), 7.44 – 7.34 (m, 1H), 7.17 (d, J = 9.5 Hz, 2H), 6.90 – 6.86 (m, 2H), 6.73 (d, J = 2.4 Hz, 2H), 4.41 (s, 2H), 3.67 – 6.57 (m, 8H), 3.28 (q, J = 6.9 Hz, 2H), 1.87 (s, 3H), 1.33 (t, J = 7.0 Hz, 12H), 1.21 (t, J = 7.1 Hz, 3H). ^{13}C NMR (150 MHz, $CDCl_3$) δ = 169.0, 157.7, 155.7, 155.1, 154.2, 135.4, 132.0, 130.4, 130.2, 126.6, 114.0, 113.7, 112.6, 96.3, 46.2, 44.5, 37.9, 13.8, 12.7, 7.8. ESI-MS $[M]^+$: *m/z* 582.7. HPLC purity ≥ 95% (CH_3CN 0.1% TFA/H_2O 0.1% TFA 70:30 (v/v), flow = 1.0 mL/min, t_R = 9.3 min), at 226, 254 and 580 nm.

3-Carbamoyl-4-((ethylamino)methyl)-1,2,5-oxadiazole 2-oxide (**15**). A solution of 4-(bromomethyl)-3-carbamoyl-1,2,5-oxadiazole 2-oxide **13** (4.50 mmol, 1 g)[37] in CH_3CN (12 mL) was treated with an excess of an ethylamine solution 70 wt% in H_2O (22.5 mmol, 1.81 mL) for 2 h at room temperature. After the reaction was complete, the mixture was extracted with DCM, washed with H_2O, brine and dried over anhydrous Na_2SO_4. The organic layer was concentrated to dryness to give target compound **15** (502 mg, 60%). ^{1}H NMR (600 MHz, $CDCl_3$) δ = 4.08 (s, 2H), 2.68 (q, J = 7.1 Hz, 2H), 1.95 (s, 1H), 1.12 (t, J = 7.1 Hz, 3H). ^{13}C NMR (150 MHz, $CDCl_3$) δ = 157.0, 156.8, 111.1, 44.7, 43.1, 15.1.

4-((2-Bromo-N-ethylbenzamido)methyl)-3-carbamoyl-1,2,5-oxadiazole 2-oxide (**6**). The intermediate **17** (2.29 mmol, 501 mg) was dissolved in dry DCM (15 mL), and compound **15** (1.8 mmol, 335 mg) and an excess of triethylamine (0.7 mL) were added and the resulting solution was stirred for 2 h. The reaction mixture was washed with a saturated sodium bicarbonate solution (2 × 15 mL), water (2 × 15 mL) and 1 M HCl (2 × 15 mL), then dried over anhydrous Na_2SO_4 and concentrated to dryness. Purification of the residue via silica gel chromatography, using DCM/Acetone (96/4, v/v) as the eluent, gave the target compound **6** as a white solid (300 mg, 65%). The ^{1}H and ^{13}C NMR spectra of the compound showed the presence of two rotamers, which are caused by the carbamoyl function. ^{1}H NMR (600 MHz, $CDCl_3$) δ = 7.62 – 7.58 (m, 1H), 7.42 – 7.37 (m, 1H), 7.36 – 7.33 (m, 1H), 7.32 – 7.28 (m, 1H), 6.06 (s) & 5.97 (s) (2H), 5.25 (d, J = 17.4 Hz) & 4.92 (d, J = 17.5 Hz) (1H), 4.85 (d,

$J = 18.4$ Hz) & 4.61 (d, $J = 18.5$ Hz) (1H), 3.43 – 3.29 (m) & 3.26 – 3.21 (m) (2H), 1.32 (t, $J = 7.1$ Hz) & 1.16 (t, $J = 7.2$ Hz) (3H). ^{13}C NMR (150 MHz, $CDCl_3$) δ = 169.7, 156.3, 155.4, 137.7 & 137.5, 133.1 & 133.0, 130.8 & 130.6, 128.1 & 128.0, 127.8 & 127.7, 119.3 & 119.2, 111.0, 44.8 & 44.4, 41.0, 14.0 & 12.4. ESI-MS $[M + H]^+$: *m/z* 369.3 and $[M + H + 2]^+$: *m/z* 371.3. HPLC purity ≥ 95% (CH_3CN 0.1% TFA/H_2O 0.1% TFA 70:30 (v/v), flow = 1.0 mL/min, t_R = 4.2 min), at 226 and 254 nm.

3-Carbamoyl-4-((2-(6-(diethylamino)-3-(diethyliminio)–3H-xanthen-9-yl)-N-ethylbenzamido)methyl)-1,2,5-oxadiazole 2-oxide (**2**). A solution of N-(9-(2-(chlorocarbonyl)phenyl)-6-(diethylamino)–3H-xanthen-3-ylidene)-*N*-ethylethanaminium (1.29 mmol, 642 mg) [25] in dry DCM (30 mL) was treated with compound **15** (240 mg, 1.29 mmol) and an excess of triethylamine (0.5 mL), and the resulting solution was stirred overnight. The reaction mixture was washed with saturated sodium bicarbonate solution (2 × 15 mL), water (2 × 15 mL) and 1 M HCl (2 × 15 mL), then dried over anhydrous Na_2SO_4 and concentrated to dryness. Purification of the residue via silica gel chromatography, using DCM/MeOH (98/2, v/v) as the eluent, gave target compound **2** as a mirrored purple solid (144 mg, 18%). ^{1}H and ^{13}C NMR spectra of the compound showed the presence of two rotamers, which are caused by the carbamoyl function.^{1}H NMR (600 MHz, $CDCl_3$) δ = 7.71 – 7.64 (m, 2H), 7.63 – 7.59 (m, 1H), 7.38 – 7.35 (m, 1H), 7.20 (d, $J = 9.5$ Hz, 2H), 6.95 – 6.89 (m, 2H), 6.87 – 6.83 (m, 2H), 4.63 (s) & 4.58 (s) (2H), 3.73 – 3.55 (m, 8H), 3.31 – 3.28 (m) & 3.21 – 3.16 (m) (2H), 1.67 (bs, 2H), 1.31 (t, J = 7.0 Hz, 12H), 1.06 (t, $J = 7.1$ Hz) & 0.78 (t, $J = 7.0$ Hz) (3H). ^{13}C NMR (150 MHz, $CDCl_3$) δ = 169.6, 157.8, 155.6, 155.4, 154.5, 153.8, 136.1, 132.0, 130.4, 130.0, 129.8, 127.3, 113.8, 113.7, 110.6, 96.7, 46.2, 45.3, 40.4, 13.9, 12.7. ESI-MS $[M]^+$: *m/z* 611.6. HPLC purity ≥ 95% (CH_3CN 0.1% TFA/H_2O 0.1% TFA 70:30 (v/v), flow = 1.0 mL/min, t_R = 7.1 min), at 226, 254 and 580 nm.

4-((2-Bromo-N-ethylbenzamido)methyl)-3-cyano-1,2,5-oxadiazole 2-oxide (**7**). Trifluoroacetic anhydride (2.04 mmol, 0.290 mL) and pyridine (1.02 mmol, 0.083 mL) were added to a solution of compound **6** (1.02 mmol, 377 mg) in dry DCM (20 mL), under positive N_2 pressure at 0 °C. The resulting solution was stirred for 3 h and subsequently washed with saturated sodium bicarbonate solution (2 × 15 mL), water (1 × 15 mL) and brine (1 × 15 mL). The organic layer was dried over anhydrous Na_2SO_4 and concentrated to dryness. The purification of the residue via silica gel chromatography, using petroleum ether/EtOAc (80/20, v/v) as the eluent, gave target compound **7** as a white solid (144 mg, 40%). ^{1}H and ^{13}C NMR spectra of the compound showed the presence of two rotamers, which are caused by the carbamoyl function. ^{1}H NMR (600 MHz, $CDCl_3$) δ = 7.62 – 7.58 (m, 1H), 7.42 – 7.37 (m, 1H), 7.36 – 7.33 (m, 1H), 7.32 – 7.28 (m, 1H) 4.96 (d, $J = 15.2$ Hz, 1H), 4.71 (d, $J = 15.2$ Hz, 1H), 3.45 – 3.28 (m) & 3.24 – 3.18 (m) (2H), 1.33 (t, J = 7.1H) & 1.19 (t, $J = 7.2$ Hz) (3H). ^{13}C NMR (150 MHz, $CDCl_3$) δ = 169.9, 153.9, 136.7, 133.1, 131.0, 127.9, 119.2, 105.5, 97.0, 44.8 & 43.2, 39.9, 13.9 & 11.9. ESI-MS $[M + Na]^+$: *m/z* 373.3 and $[M + Na + 2]^+$: *m/z* 375.3. HPLC purity ≥ 95% (CH_3CN 0.1% TFA/H_2O 0.1% TFA 70:30 (v/v), flow = 1.0 mL/min, t_R = 5.06 min), at 226 and 254 nm.

3-Cyano-4-((2-(6-(diethylamino)-3-(diethyliminio)–3H-xanthen-9-yl)-N-ethylbenzamido)methyl)-1,2,5-oxadiazole 2-oxide (**3**). Trifluoroacetic anhydride (0.346 mmol, 0.050 mL) and pyridine (0.173 mmol, 0.017 mL) were added to a solution of compound **2** (0.173 mmol, 112 mg) in dry DCM (15 mL), under positive N_2 pressure at 0 °C. The resulting solution was stirred for 3 h and subsequently washed with a saturated sodium bicarbonate solution (2 × 15 mL), water (2 × 15 mL) and brine (2 × 15 mL). The organic layer was dried over anhydrous Na_2SO_4 and concentrated to dryness. Purification of the residue via silica gel chromatography, using DCM/MeOH (98/2, v/v) as the eluent, gave target compound **3** as a mirrored purple solid (54 mg, 50%). ^{1}H NMR (600 MHz, $CDCl_3$) δ = 7.74 – 7.69 (m, 2H), 7.62 – 7.59 (m, 1H), 7.41 – 7.38 (m, 1H), 7.20 (d, $J = 9.5$ Hz, 2H), 6.98 – 6.94 (m, 2H), 6.72 (d, $J = 2.4$ Hz, 2H), 4.50 (s, 2H), 3.69 – 3.55 (m, 8H), 3.36 (q, $J = 6.9$ Hz, 2H), 1.32 (t, $J = 7.0$ Hz, 12H), 1.22 (t, $J = 7.0$ Hz, 3H). ^{13}C NMR (150 MHz, $CDCl_3$) δ = 169.4, 157.7, 155.7, 155.0, 152.9, 132.0, 130.5, 130.4, 130.3, 126.8, 114.3, 113.6, 105.0, 97.0, 96.2, 46.2, 45.1, 39.0, 13.9, 12.6. ESI-MS $[M]^+$: *m/z* 593.5. HPLC purity ≥ 95% (CH_3CN 0.1% TFA/H_2O 0.1% TFA 70:30 (v/v), flow = 1.0 mL/min, t_R = 9.5 min), at 226, 254 and 580 nm.

2-Bromo-N-ethyl-N-(2-hydroxyethyl)benzamide (**19**). Intermediate **17** (2.29 mmol, 501 mg), dissolved in dry DCM (15 mL), was treated with 2-(ethylamino)ethanol (22.9 mmol, 2.24 mL) and stirred for 3 h at room temperature. After the reaction was complete, the mixture was washed with water (2 × 15 mL), a saturated sodium bicarbonate solution (2 × 15 mL) and 1 M HCl (2 × 15 mL), then dried over anhydrous Na_2SO_4. The organic layer was concentrated to dryness to give target compound **19** (311 mg, 50%). ^{1}H and ^{13}C NMR spectra of the compound showed the presence of two rotamers, which are caused by the carbamoyl function. ^{1}H NMR (600 MHz, $CDCl_3$) δ = 7.59 – 7.56 (m) & 7.54 – 7.52 (m) (1H), 7.37 – 7.30 (m, 1H), 7.28 – 7.19 (m, 2H), 3.94 – 3.88 (m) & 3.88 – 3.81 (m) (2H), 3.67 – 3.51 (m, 1H), 3.38 – 3.29 (m) & 3.28 – 3.16 (m) (2H), 1.26 (t, $J = 7.1$ Hz) & 1.07 (t, $J = 7.2$ Hz) (3H). ^{13}C NMR (150 MHz, $CDCl_3$) δ = 170.9 & 169.3, 138.5 & 138.2, 133.0 & 132.8, 130.5 & 130.2, 128.3 & 127.8, 127.7 & 127.6, 119.3 & 119.3, 62.2 & 60.3, 49.9 & 48.5, 45.2 & 40.2, 14.0 & 12.4.

4-(2-(2-Bromo-N-ethylbenzamido)ethoxy)-3-(phenylsulfonyl)-1,2,5-oxadiazole 2-oxide (**8**). 3,4-bis(phenylsulfonyl)furoxan **20** (1.10 mmol, 403 mg) and 1,8-diazabicyclo[5.4.0]undec-7-ene (2.20 mmol, 0.328 mL) were added to a solution of compound **19** (1.10 mmol, 300 mg) in dry DCM (10 mL). The resulting mixture was stirred for 4 h at room temperature, subsequently washed with water (3 × 15 mL) and dried over anhydrous Na_2SO_4. The organic layer was concentrated to dryness. The crude product was purified via silica gel chromatography using DCM/Acetone (98/2, v/v) and the desired compound **8** was obtained as a colourless oil (430 mg, 79%). ^{1}H and ^{13}C NMR spectra of the compound showed the presence of two rotamers, which are caused by the carbamoyl function. ^{1}H NMR (600 MHz, $CDCl_3$) δ = 8.08 – 8.02 (m, 1H), 7.80 – 7.73 (m, 1H), 7.67 – 7.54 (m, 1H), 7.43 – 7.37 (m, 1H), 4.85 – 4.70 (m) & 4.52 – 4.45 (m) & 4.42 – 4.35 (m) (2H), 4.20 – 4.12 (m) & 4.08 – 4.01 (m) (1H), 3.90 – 3.82 (m) & 3.76 – 3.69 (m) (1H), 3.63 – 3.56 (m) & 3.50 – 3.42 (m) & 3.36 – 3.29 (m) (1H), 1.34 (t, $J = 7.1$ Hz) & 1.15 (t, $J = 7.1$ Hz) (3H). ^{13}C NMR (150 MHz, $CDCl_3$) δ = 169.6, 158.9, 138.1 & 137.90, 136.0 & 135.8, 133.0 & 132.9, 130.6 & 130.5, 129.9 & 129.8, 128.8 & 128.7, 128.3 & 128.0, 127.9 & 127.6, 119.3, 110.7, 69.4 & 68.89, 46.0 & 45.0, 43.4 & 40.4, 14.16 & 12.5. ESI-MS $[M + H]^+$: *m/z* 496.3 and $[M + H + 2]^+$: *m/z* 498.3. HPLC purity ≥ 95% (CH_3CN 0.1% TFA/H_2O 0.1% TFA 70:30 (v/v), flow = 1.0 mL/min, t_R = 7.0 min), at 226 and 254 nm.

4-(2-(2-(6-(Diethylamino)-3-(diethyliminio)–3H-xanthen-9-yl)-N-ethylbenzamido)ethoxy)-3-(phenylsulfonyl)-1,2,5-oxadiazole 2-oxide (**4**). A solution of *N*-(9-(2-(chlorocarbonyl)phenyl)-6-(diethylamino)–3H-xanthen-3-ylidene)-*N*-ethylethanaminium **18** (0.96 mmol, 477 mg) [25] in dry DCM (10 mL) was treated with 2-(((3-phenylsulfonylfuroxan-4-yl) oxy)ethyl)ethylamine **24** (0.96 mmol, 300 mg) [38] and an excess of triethylamine (0.4 mL), and the resulting solution was stirred for 24 h. The reaction mixture was washed with water (2 × 15 mL) and a saturated sodium bicarbonate solution (4 × 15 mL), then dried over anhydrous Na_2SO_4 and concentrated to dryness. Purification of the residue via silica gel chromatography, using DCM/Acetone (80/20, v/v) as the eluent, gave target compound **4** as a mirrored purple solid (200 mg, 27%). ^{1}H and ^{13}C NMR spectra of the compound showed the presence of two rotamers, which are caused by the carbamoyl function. ^{1}H NMR (600 MHz, $CDCl_3$) δ = 8.05 (d, $J = 7.8$ Hz) & 7.99 (d, $J = 7.7$ Hz) & 7.93 (d, $J = 7.7$ Hz) (2H), 7.78 – 7.67 (m) & 7.65 – 7.60 (m) (6H), 7.38 – 7.29 (m, 3H), 6.95 – 6.90 (m) & 6.80 – 6.74 (m) (2H), 6.70 (d, $J = 2.1$ Hz, 2H), 3.99 (t, $J = 4.8$ Hz, 2H), 3.72 – 3.55 (m, 8H), 3.33 (q, $J = 6.9$ Hz, 2H), 1.34 – 1.23 (m, 12H), 1.17 (t, $J = 7.0$ Hz) & 0.63 (t, $J = 6.9$ Hz) (3H). ^{13}C NMR (150 MHz, $CDCl_3$) δ = 169.3, 158.4, 157.7, 155.7, 137.8, 136.1 & 136.0, 132.3, 130.6 & 130.6, 130.1 & 130.0, 129.9, 128.6, 128.3, 127.2, 114.2, 113.4, 110.3, 96.4 and 96.2, 69.6 & 69.5, 53.9, 46.2 & 45.5, 43.0, 31.9 & 31.1, 29.4, 14.2, 12.7. ESI-MS $[M]^+$: *m/z*

738.6. HPLC purity ≥ 95% (CH_3CN 0.1% TFA/H_2O 0.1% TFA 70:30 (v/v), flow = 1.0 mL/min, t_R = 10.4 min), at 226, 254 and 580 nm.

4-(2-Aminoethoxy)-3-(phenylsulfonyl)-1,2,5-oxadiazole-2-oxide (**21**). Ethanolamine (3.0 mmol, 0.180 mL) and sodium hydride (2.0 mmol, 80 mg) at 0 °C were added to a solution of 3,4-bis(phenylsulfonyl)furoxan **20** (1.0 mmol, 366 mg) in anhydrous THF (15 mL). The solution was slowly warmed to room temperature and stirred for 2 h. The reaction mixture was concentrated *in vacuo*, dissolved in 15 mL of water and extracted with EtOAc (3 × 10 mL). The organic layer was collected, washed with water (25 mL) and brine (25 mL) sequentially, then dried over anhydrous Na_2SO_4 and concentrated to dryness. The crude product was purified via silica gel chromatography using DCM/MeOH (NH_3 sat) (90/10, v/v) and the desired compound **21** was obtained as a white solid (60 mg, 56%). ^{1}H NMR (600 MHz, $CDCl_3$) δ = 8.08 – 8.05 (m, 2H), 7.79 – 7.74 (m, 1H), 7.65 – 7.60 (m, 2H), 4.46 (t, J = 5.2 Hz, 2H), 3.20 – 3.17 (m, 2H), 1.25 (bs, 2H). ^{13}C NMR (150 MHz, $CDCl_3$) δ = 159.1, 138.1, 135.8, 129.8, 128.7, 73.6, 40.8.

(Z)-4-Carboxy-N-(9-(diethylamino)-5H-benzo[a]phenothiazin-5-ylidene)butan-1-aminium (**23**). (Z)-*N*-(9-(diethylamino)-5H-benzo[*a*]phenothiazin-5-ylidene)-5-ethoxy-5-oxopentan-1-aminium **22** was synthesised as described by Sarika Verma *et al.* [39] starting from the respective naphthyl derivative (0.59 mmol, 308 mg). Intermediate **22** was dissolved in a solution of dioxane/6 M HCl (50/50, v/v, 12 mL) and kept under stirring at room temperature overnight. The solvent was evaporated and the residue was taken up with DCM (20 mL), and concentrated under reduced pressure twice. The crude product was purified via silica gel chromatography using DCM/MeOH (95/5, v/v) and the desired compound **23** was obtained as a blue solid (40 mg, 15%). ^{1}H NMR (600 MHz, CD_3OD) δ = 8.43 – 8.31 (m, 1H), 8.04 – 7.90 (m, 1H), 7.62 – 7.43 (m, 3H), 7.19 – 6.99 (m, 1H), 6.89 – 6.64 (m, 2H), 3.61 – 3.53 (m, 4H), 3.40 – 3.32 (m, 2H), 2.36 – 2.28 (m, 2H), 1.79 – 1.68 (m, 54), 1.32 – 1.21 (m, 6H). ^{13}C NMR (150 MHz, CD_3OD) δ = 179.7, 152.8, 151.1, 130.7, 129.2, 124.6, 123.9, 117.1, 104.6, 101.7, 99.4, 45.5, 44.0, 35.9, 27.9, 23.1, 11.9.

(Z)-4-(2-(5-((9-(Diethylamino)-5H-benzo[a]phenothiazin-5-ylidene) ammonio)pentanamido)ethoxy)-3-(phenylsulfonyl)-1,2,5-oxadiazole 2-oxide (**10**). *N*-(3-dimethylaminopropyl)-*N*′-ethylcarbodiimide hydrochloride (EDC·HCl, 0.55 mmol, 106 mg), 1-hydroxybenzotriazole hydrate (HOBt, 0.63 mmol, 89 mg), 4-(dimethylamino)pyridine (DMAP, 0.55 mmol, 69 mg) and intermediate **21** (0.55 mmol, 157 mg) were added to a solution of compound **23** (0.42 mmol, 197 mg) in dry DMF (20 mL). The resulting mixture was stirred for 24 h at room temperature and subsequently concentrated to dryness. Purification of the residue via silica gel chromatography, using DCM/MeOH (97/3, v/v) as the eluent, gave the target compound **10** as a blue solid (155 mg, 50%). ^{1}H NMR (600 MHz, $CDCl_3$) δ = 8.96 – 8.91 (m, 1H), 8.78 (d, J = 8.1 Hz, 1H), 8.11 – 8.04 (m, 2H), 7.96 (d, J = 9.4 Hz, 1H), 7.78 – 7.66 (m, 3H), 7.60 (t, J = 7.8 Hz, 2H), 7.13 – 7.09 (m, 1H), 7.03 (s, 1H), 6.85 (d, J = 2.7 Hz, 1H), 4.53 (t, J = 5.6 Hz, 2H), 3.84 – 3.78 (m, 2H), 3.75 (q, J = 5.6 Hz, 2H), 3.61 (q, J = 7.2 Hz, 4H), 2.48 (t, J = 7.3 Hz, 2H), 1.99 – 1.91 (m, 2H), 1.91 – 1.84 (m, 2H), 1.35 (t, J = 7.2 Hz, 6H). ^{13}C NMR (150 MHz, $CDCl_3$) δ = 173.8, 158.8, 154.5, 148.4, 137.9, 135.7, 134.3, 133.1, 129.8, 129.5, 128.6, 124.7, 124.0, 110.5, 105.1, 70.4, 44.9, 38.1, 36.3, 30.2, 23.8, 12.8. ESI-MS $[M]^+$: m/z 701.7. HPLC purity ≥ 95% (CH_3CN 0.1% TFA/H_2O 0.1% TFA 80:20 (v/v), flow = 1.2 mL/min, t_R = 11.1 min), at 226, 254 and 660 nm.

(Z)-N-(9-(Diethylamino)-5H-benzo[a]phenothiazin-5-ylidene)-5-(ethylamino)-5-oxopentan-1-aminium (**11**). *N*-(3-dimethylaminopropyl)-*N*′-ethylcarbodiimide hydrochloride (EDC·HCl, 0.17 mmol, 32 mg), 1-hydroxybenzotriazole hydrate (HOBt, 0.19 mmol, 26 mg), 4-(dimethylamino)pyridine (DMAP, 0.17 mmol, 21 mg) and a 2 M ethylamine solution in THF (0.64 mmol, 34 μL) were added to a solution of compound **23** (0.13 mmol, 60 mg) in dry DMF (10 mL). The resulting mixture was stirred for 24 h at room temperature and subsequently concentrated to dryness. Purification of the residue via silica gel chromatography, using DCM/MeOH (98/2, v/v) as the eluent, gave the target compound **11** as a blue solid (55 mg, 86%). ^{1}H NMR (600 MHz, CD_3OD) δ = 8.82 (d, J = 8.1 Hz, 1H), 8.20 (d, J = 8.1 Hz, 1H), 7.83 (d, J = 9.4 Hz, 1H), 7.79 (t, J = 7.5 Hz, 1H), 7.63 – 7.68 (m, 1H), 7.30 – 7.26 (m, 1H), 7.13 (s, 1H), 7.09 (d, J = 2.7 Hz, 1H), 3.66 (q, J = 7.2 Hz, 4H), 3.60 (t, J = 6.9 Hz, 2H), 3.25 – 3.16 (m, 2H), 2.33 (t, J = 7.0 Hz, 2H), 1.88 – 1.72 (m, 4H), 1.34 (t, J = 7.2 Hz, 6H), 1.13 (t, J = 7.3 Hz, 3H). ^{13}C NMR (150 MHz, CD_3OD) δ = 175.5 & 175.4, 154.6, 152.7, 141.4, 138.5, 135.2, 134.8, 134.1, 133.3, 132.2, 130.8, 126.3, 125.5, 123.5, 118.7, 106.1, 103.3, 46.9, 45.2, 36.3, 35.4 & 35.2, 29.1, 24.3, 14.9, 13.1. ESI-MS $[M]^+$: m/z 461.6. HPLC purity ≥ 95% (CH_3CN 0.1% TFA/H_2O 0.1% TFA 80:20 (v/v), flow = 1.2 mL/min, t_R = 16.9 min), at 226, 254 and 660 nm.

2.2. Determination of lipophilicity descriptor (log P)

The partition coefficients (log P), between *n*-octanol and PBS (pH 7.4), of the target and reference compounds were obtained using the shake-flask technique at room temperature. In the shake-flask experiments, 50 mM PBS (pH 7.4) was used as the aqueous phase and ionic strength was adjusted to 0.15 M using KCl. The organic (*n*-octanol), and aqueous phases were mutually saturated via shaking for 4 h. The compounds were solubilised in the buffered aqueous phase at concentrations of either 0.1 mM or 0.05 mM, depending on their solubility, and appropriate amounts of *n*-octanol were added. The two phases were shaken for about 20 min, by which time the partitioning equilibrium of the solutes had been reached, and then centrifuged (10000 rpm, 10 min). The concentration of the solutes was measured in the aqueous phase using a UV spectrophotometer (UV-2501PC, Shimadzu). Each log P value is an average of at least six measurements. All experiments were performed avoiding exposure to light.

2.3. NO release in physiological solution

NO release was evaluated as nitrite, produced during incubation in the following conditions, and detected using the Griess reaction. All of the compounds, except derivative **10**, were incubated at 100 μM in a mixture 50 mM pH 7.4 PBS solution/MeOH (1% DMSO) 50/50 v/v. The compound with lysosomal targeting, **10**, and its non-targeted reference, **8**, however, were incubated at 100 μM in a mixture 50 mM pH 5.0 citrate buffer solution / MeOH (1% DMSO) 50/50 v/v. The incubation of all compounds was performed in the presence of L-cysteine at a 0.5 mM concentration (a 5-fold excess compared to the NO-donor derivative). After 1 h at 37 °C, the presence of nitrite in the sample was determined using the Griess assay: 1 mL of the reaction mixture was treated with 250 μL of the Griess reagent (4% w/v sulphanilamide, 0.2% w/v *N*-naphthylethylenediamine dihydrochloride, 1.47 M phosphoric acid); after 10 min at room temperature, the reaction mixture was analysed via RP-HPLC to detect the azo dye.

HPLC analyses were performed using a HP 1200 chromatograph system (Agilent Technologies, Palo Alto, CA, USA) equipped with a quaternary pump (model G1311A), a membrane degasser (G1322A), and a multiple wavelength UV detector (MWD, model G1365D) integrated into the HP1200 system. Data analysis was performed using a HP ChemStation system (Agilent Technologies). The sample was eluted on a HyPURITY Elite C_{18} column (250 × 4.6 mm, 5 μm, Hypersil, ThermoQuest Corporation, UK). The injection volume was 20 μL (Rheodyne, Cotati, CA). The mobile phase consisted of CH_3CN 0.1% TFA (solvent A) and H_2O 0.1% TFA (solvent B) at flow-rate = 1.0 mL/min with gradient conditions: 50% A to 4 min; from 50 to 90% A between 4 and 8 min; 90% A between 8 and 12 min; and from 90 to 50% A between 12 and 15 min. The column effluent was monitored at 540 mn and referenced against a 800 nm wavelength. Data analysis was performed using Agilent ChemStation. The values obtained from the integration of the peak of azo dye were interpolated in a calibration curve obtained using standard solutions of sodium nitrite at 0.5 μM to 50 μM (r^2 = 0.996). The yield in nitrite was expressed as percentage NO_2^- (mol/mol, relative to the initial compound concentration) ± SEM.

2.4. UPLC-MS analysis

In order to detect the products formed in the reaction between the furoxan derivatives and L-cysteine, hybrid compounds **3** and **4** were incubated at 100 μM in a mixture of 50 mM pH 7.4 PBS solution/MeOH (1% DMSO) 50/50 v/v. The incubation of the two compounds was performed at 37 °C in the presence of L-cysteine at a 0.5 mM concentration (a 5-fold excess compared to the NO-donor derivative). At regular time intervals, the reaction mixture was filtered through a 13 mm Syringe Filter w/0.45 μm polytetrafluoroethylene membrane and the filtrate was analysed on a Acquity Ultra Performance LC, Waters Corporation Milford MA, USA, equipped with BSM, SM, CM and a PDA detector. The analytical column was a Phenomenex Synergi 4U POLAR-RP80A, 150 × 2 mm·4 μm. The mobile phase consisted of CH_3CN 0.1% HCOOH and H_2O 0.1% HCOOH 80/20 v/v. The UPLC retention time (t_R) was obtained at a flow rate of 0.4 mL min^{-1}, and the column effluent was monitored using a Micromass Quattro micro API, with Esci multimode ionisation enabled, as the detector. The molecular ion $[M]^+$ was employed for quantitative measurements of the analytes. The MS conditions were: drying gas (nitrogen) heated at 350 °C at a flow rate of 800 L/h; nebuliser gas (nitrogen) at 80 L/h; capillary voltage in positive mode at 3000 V; fragmentor voltage at 30.

3. Biological studies

3.1. Chemicals

Cell culture medium was supplied by Invitrogen Life Technologies (Carlsbad, CA) and plasticware for cell cultures was obtained from Falcon (Becton Dickinson, Franklin Lakes, NJ). The protein content of cell monolayers and lysates was assessed using the BCA kit from Sigma Chemical Co (St. Louis, MO). Unless otherwise specified, all reagents were obtained from Sigma Chemical Co. A 5 mM stock solution in DMSO was prepared for all compounds; this stock solution was diluted in culture medium to achieve the final concentration. The concentration of DMSO in the culture medium was<0.1% under each experimental condition. Control cells were treated with 0.1% DMSO. Preliminary experiments showed that cells treated with 0.1% DMSO did not differ from cells treated with culture medium without DMSO in any biological assay (data not shown).

3.2. Cells

Human lung adenocarcinoma A549 cells, provided by Istituto Zooprofilattico Sperimentale "Bruno Ubertini" (Brescia, Italy), were cultured in Ham's F12 medium supplemented with 10% foetal bovine serum and 1% penicillin–streptomycin. Cell cultures were maintained in a humidified atmosphere at 37 °C and 5% CO_2. When indicated, cells were incubated for 24 h with the compounds in Ham's F12 before the experimental procedures described below.

3.3. NO release in cells

After incubation, 1 mL of cell supernatant was collected, centrifuged for 10 min at 13000g, and then the presence of nitrite in the reaction mixture was determined using the Griess assay: 0.5 mL of the reaction mixture was treated with 125 μL of the Griess reagent (4% w/v sulphanilamide, 0.2% w/v *N*-naphthylethylenediamine dihydrochloride, 1.47 M phosphoric acid); after 10 min at room temperature, the sample was analysed using RP-HPLC to detect the azo dye, as previously described in paragraph 2.3.

3.4. Cytotoxicity

The cytotoxic effect of the compounds was measured as the leakage of lactate dehydrogenase (LDH) activity into the extracellular medium

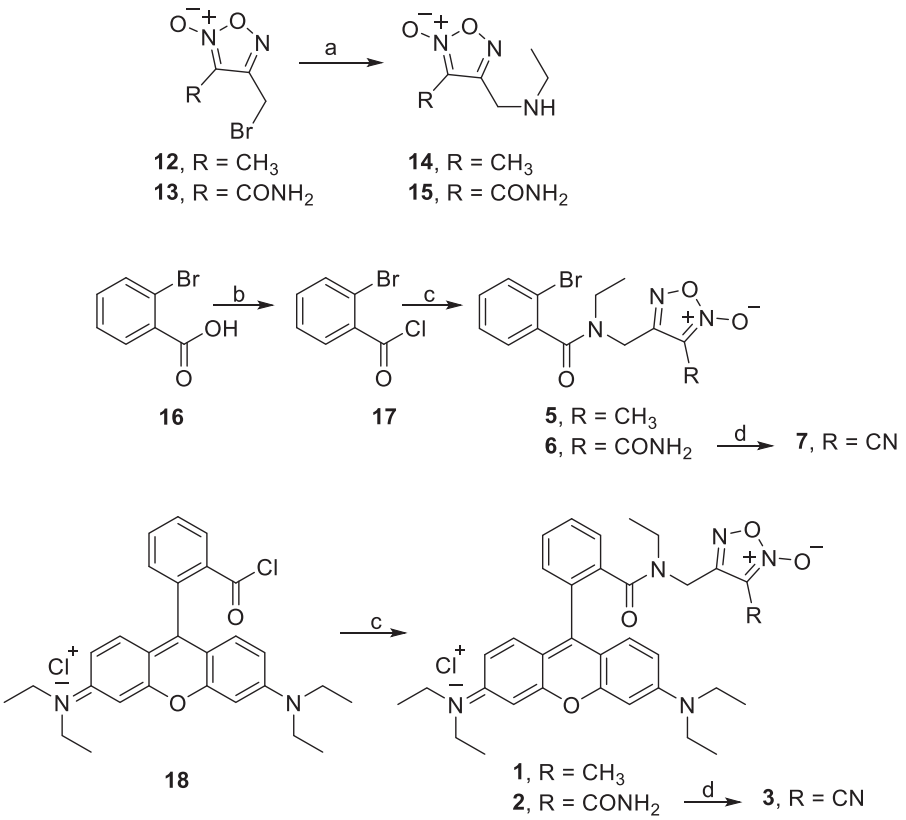

Scheme 1. Synthesis of target compounds **1**–**3** and related reference compounds **5**–**7**. Reagents and conditions: a) $CH_3CH_2NH_2$ 70% wt. in H_2O, CH_3CN, rt; b) $SOCl_2$, DCM, Δ; c) **14** or **15**, Et_3N, DCM, rt; d) $(CF_3CO)_2O$, pyridine, dry DCM, 0 °C.

using a Synergy HT microplate reader (Bio-Tek Instruments, Winooski, VT) [40]. This method is a sensitive index of cell necrosis – the type of cell death expected from a damage in lysosome and mitochondria – verified in different cancer types treated with antitumor agents releasing NO [17,24,25,41]. Both intracellular and extracellular LDH were measured, and the extracellular LDH activity (LDH out) was calculated as a percentage of the total (intracellular + extracellular) LDH activity (LDH tot) in the dish. All compounds were tested in a concentration range 0.1–50 μM, except for compounds **10** and **11**, due to their poor solubility in the cellular medium at 50 μM.

3.5. Intracellular localisation studies

5×10^5 A549 cells were grown on sterile glass coverslips and transfected with the GFP-E1α pyruvate dehydrogenase expression vector (CellLight™ Mitochondria-GFP, BacMam 2.0, Invitrogen Life Technologies) to label mitochondria, or with the GFP-Lamp1 expression vector (CellLight™ Lysosomes-GFP, BacMam 2.0, Invitrogen Life Technologies) to label lysosomes. After 24 h, mitochondrion-labelled cells were incubated with 5 μM of either compound **3** or compound **4** for 4 h, and lysosome-labelled cells with 5 μM of compound **10** for 4 h. Samples were then rinsed with PBS, fixed with 4% w/v paraformaldehyde for 15 min, washed three times with PBS and once with water, and mounted with 4 μL of Gel Mount Aqueous Mounting. For compound **3**, slides were analysed using an Olympus FV300 laser scanning confocal microscope (Olympus Biosystems, Hamburg, Germany; ocular lens: 10X; objective: 60X). For compounds **4** and **10**, slides were analysed using a Leica DC100 microscope (Leica Microsystems GmbH, Wetzlar, Germany; 10X ocular lens, 63X objective). For each experimental condition, a minimum of 5 microscopic fields were examined. The ratio of yellow pixels/green pixels (i.e., mitochondria containing compound **4**/total mitochondria or lysosomes containing compound **10**/total lysosomes) was calculated with the ImageJ software (https://imagej.nih.gov/ij/).

3.6. Statistical analysis

All data are provided as means ± SEM. The results were analysed using one-way Analysis of Variance (ANOVA) and Tukey's test (software: SPSS 21.0 for Windows, SPSS Inc., Chicago, IL). $p < 0.05$ was considered significant.

4. Results and discussion

4.1. Chemistry

The hybrid rhodamine derivative **1** and its reference compound **5** were prepared as depicted in Scheme 1. The treatment of 4-bromomethy-3-methylfuroxan (**12**) [36] with a 70% ethylamine water solution afforded the formation of 4-ethylaminoethyl-3-methylfuroxan (**14**). A dichloromethane (DCM) solution of this intermediate, containing an excess of triethylamine, was treated with acyl chloride **17**, which was, in turn, obtained from the reaction between **16** and thionyl chloride,

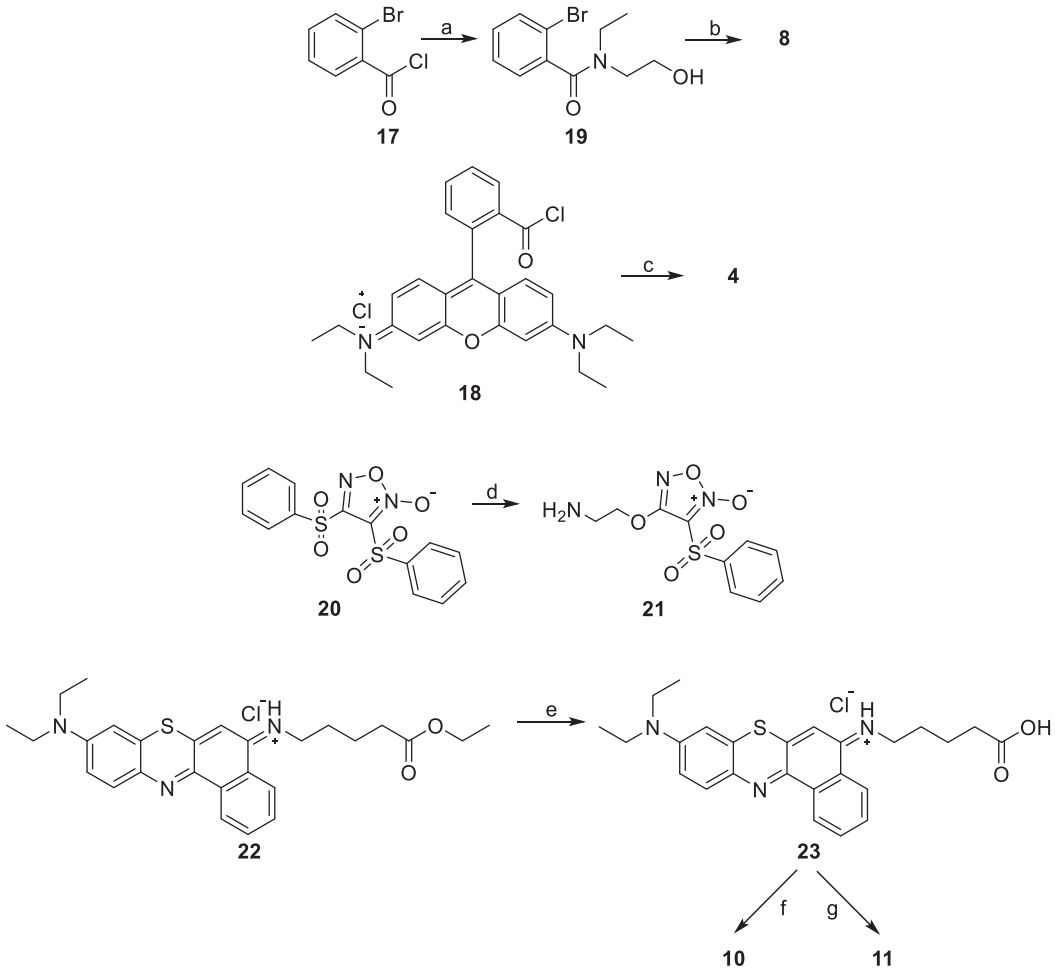

Scheme 2. Synthesis of target compounds **4**, **8**, **10** and **11**. Reagents and conditions: a) $CH_3CH_2NHCH_2CH_2OH$, DCM, rt; b) **20** (3,4-bis(phenylsulfonyl)furoxan), DBU, DCM, rt; c) **24** (2-(((3-phenylsulfonylfuroxan-4-yl)oxy)ethyl)ethylamine), Et_3N, DCM, rt; d) $NH_2CH_2CH_2OH$, NaH, THF, 0 °C; e) dioxane/6 M HCl (50/50, v/v) rt; f) **21**, EDC·HCl, HOBt, DMAP, DMF, rt; g) 2 M $CH_3CH_2NH_2$ in THF, EDC·HCl, HOBt, DMAP, DMF, rt.

Table 1
NO release and lipophilicity of the target compounds.[a]

COMPOUND	NO release	Lipophilicity	
	% NO_2^- (mol/mol) ± SEM	CLOGP[a] (BioLoom)	log P ± SEM
5	0	2.13	1.96 ± 0.02
1	0	2.24	1.90 ± 0.07
6	< 1	1.56	1.63 ± 0.06
2	< 1	1.67	1.55 ± 0.03
7	25 ± 1	2.84	2.60 ± 0.05
3	17 ± 1	2.94	2.68 ± 0.09
8	26 ± 7	4.66	nd
4	24 ± 4	4.65	nd
10	20 ± 1	6.94	nd

[a] calculated by BioLoom (BioLoom for windows v. 1.5, BioByte Corp. Claremont, CA 91711–4707); nd = not determinable by this method (log P > 4).

yielding reference product **5**. Under these same conditions, the final product **1** was prepared starting from **18** [25]. Analogous procedures were used to prepare 3-carbamoyl-4-ethylaminomethyl (**15**) from **13**, [37] and the final products **2** and **6** from **18** and **17**, respectively (Scheme 1).

The cyano-substituted final products **3** and **7** were obtained via the dehydration of the related amides **2** and **6** under the action of trifluoroacetic anhydride and pyridine in dry DCM solutions (Scheme 1).

3-Phenylsulfonylfuroxan derivatives **4** and **8** were synthesised according the pathways depicted in Scheme 2. Intermediate **17** was dissolved in dry DCM and allowed to react with an excess of 2-(ethylamino) ethanol to afford **19**. The nucleophilic displacement of the 4-phenylsulfonyl group of 3,4-diphenylfuroxan (**20**) by **19** in a dry DCM solution, in the presence of 1,8-diazabicyclo[5.4.0]undec-7-ene (DBU), gave **8**. Finally, coupling between **18** and (2-{[(3-phenylsulfonylfuroxan-4-yl) oxy]ethyl}ethylamine (**24**)[38] in dry DCM, which contained an excess of trimethylamine, produced the last derivative of our series **4**.

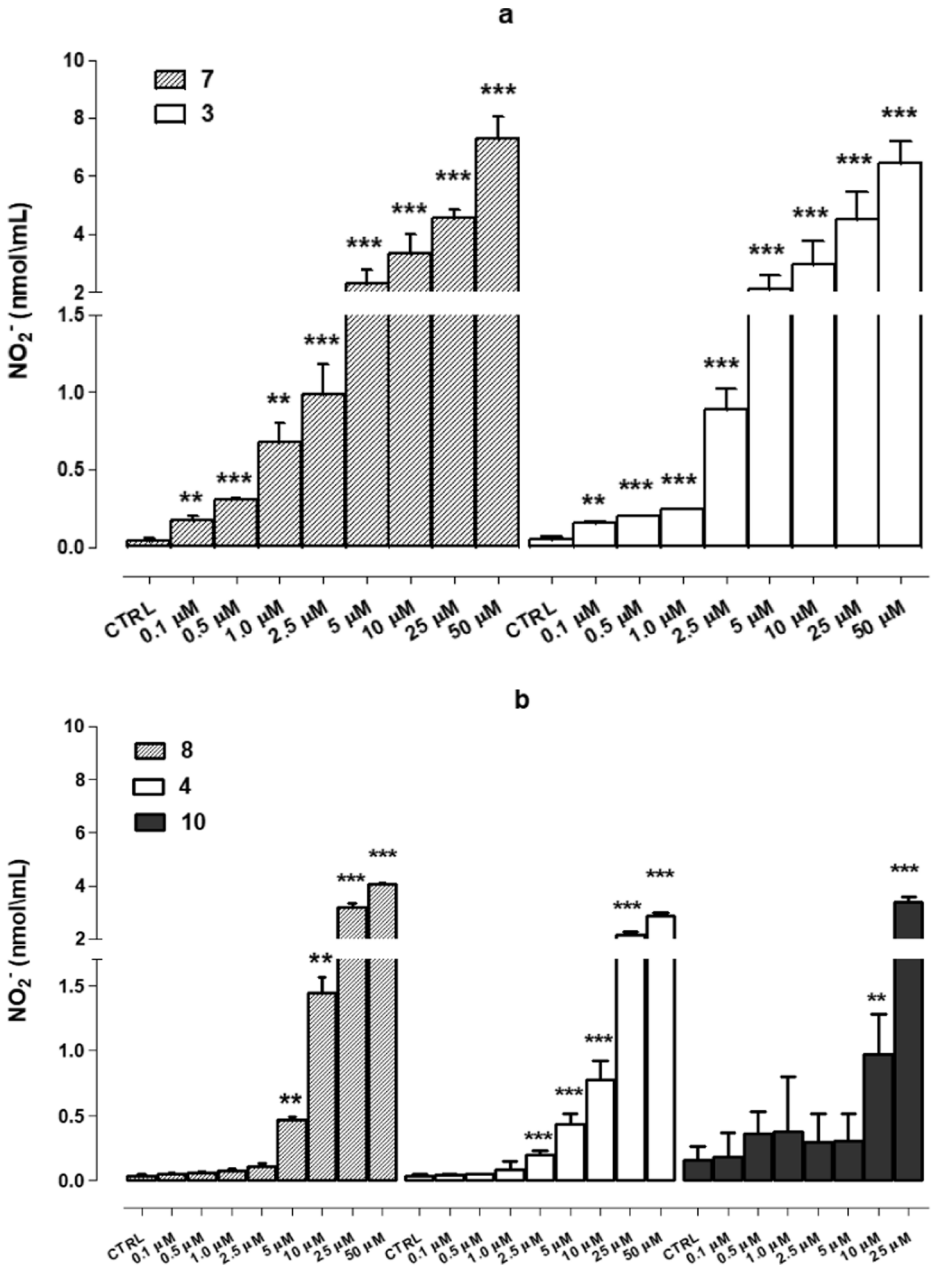

Fig. 1. a-b. NO release in A549 cells after 24 h incubation with compounds **3** vs **7** (a) and **4** vs **8** vs **10** (b). Measurements were performed in duplicate and data are presented as means ± SEM (n = 3) Vs untreated cells (CTRL): *p < 0.05; **p < 0.01, ***p < 0.001.

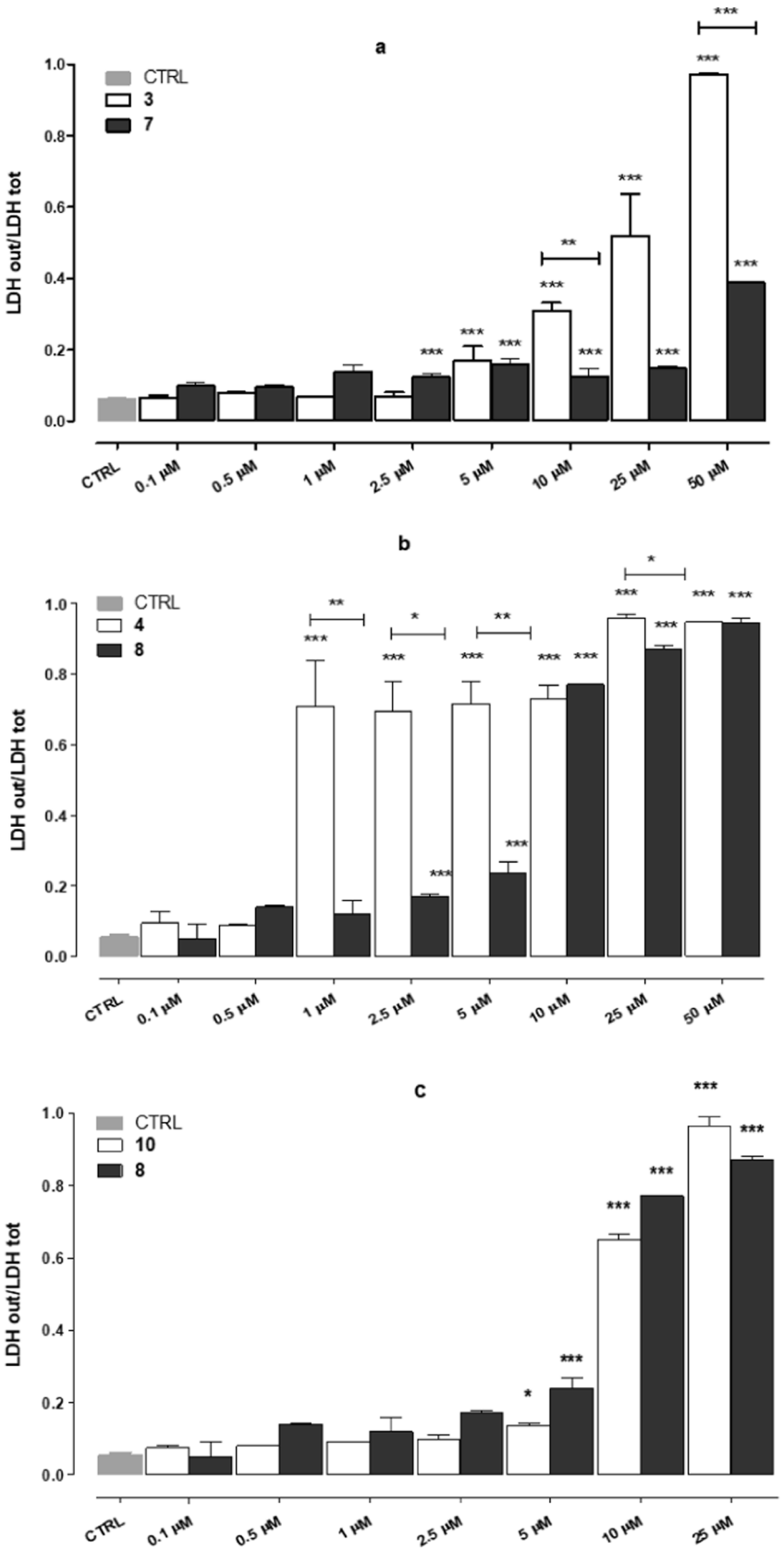

Fig. 2. a-c. Cytotoxicity of compounds **3** vs **7** (a), **4** vs **8** (b) and **10** vs **8** (c) against A549 lung adenocarcinoma cancer cells. Measurements were performed in duplicate and data are presented as means ± SEM (n = 3). Vs untreated cells (CTRL): *p < 0.05, **p < 0.01, ***p < 0.001.

The synthesis of target compounds **10** and **11**, which contain the phenothiazine chromophore, is reported in Scheme 2. The addition of 3,4-*bis* (phenylsulfonyl)furoxan (**20**) to a THF solution of ethanolamine and NaH at 0 °C generated **21**. The acid hydrolysis of the phenothiazine ester **22** carried out in dioxane gave intermediate **23** [39]. This latter, coupled with **21** in dry DMF under the action of 4-(dimethylamino) pyridine (DMAP), *N*-ethyl-*N*′-(3-dimethylaminopropyl)carbodiimide hydrochloride (EDC·HCl) and 1-hydroxybenzotriazole hydrate (HOBt), afforded **10**. Under these same conditions, the final product **11** was prepared from **23** under the action of a THF solution of ethylamine.

4.2. Lipophilicity

Lipophilicity is an important molecular descriptor that plays a leading role in the passive cellular absorption of a substance. The partition coefficient (Log P) between *n*-octanol and water is normally used to describe a product's lipophilicity [42]. Log P of the final compounds **1**–**3** and **5**–**7** was measured using the shake-flask technique and 50 mM PBS (pH 7.4) as the aqueous phase. The results are reported in Table 1 and are compared with the corresponding CLOGP values, showing a good agreement between experimental and calculated data. The compounds bearing the mitochondrial targeting moiety (**1**–**4**) displayed a hydrophilic-lipophilic balance comparable to that of the corresponding reference compounds **5**–**8**.

4.3. NO release in physiological solution

The NO-releasing capacity of all the final furoxan derivatives in the presence of thiol cofactors was evaluated in a PBS solution that contained an excess of cysteine (1:5). NO release was assessed by the detection of nitrite, the primarily product of NO/O_2 oxidation in aerobic aqueous solution, using Griess reaction. The formation of nitrite in these conditions is governed by a third-order rate law and can be accompanied by the production of a very little amount of nitrate.

The results, reported in Table 1, show that furoxans **1** and **5** did not release a detectable amount of NO after 1 h. A small amount of NO was produced by **2** and **6**, which bear the electron withdrawing carbamoyl group at position 3. By contrast, a large amount of NO was generated by **4**,**8**,**10** and **3**,**7**, in which the furoxan rings are substituted at position 3 by strongly electron withdrawing $-SO_2C_6H_5$ and –CN groups, respectively [43]. An analysis of the data also showed that the NO-releasing capacity of the organelle-targeting products **3**,**4**,**10** is comparable to that of the related references **7** and **8**.

The UPLC/mass study of the reaction of **4** with cysteine showed that a relevant amount of the corresponding 3-cysteinyl derivative is formed after 5 min (Figure S1a, see SI), in keeping with the nucleophilic displacement of the 3-phenylsulfonyl moiety in the furoxan system [44]. A thioimidate adduct between cysteine and the strong electrophilic CN group was detected, after 5 min, in an analogous UPLC/mass study carried out on **3** (Figure S2a). It is possible that the corresponding 3-thio substituted derivatives and thiocyano adducts may play some role in the NO release of the 3-phenylsulfonyl and the 3-CN furoxans, respectively.

The mechanism of NO release from furoxans in presence of thiol cofactors is complex and still needs further investigation (5a,6,7). Generally speaking, the release is favoured by basic pH and by the low pK_a of the thiol reagent, allowing thiolate anions to perform a nucleophilic attack on the hetero-ring. In Figures S1 and S2, possible mechanisms of NO production by 3-$SO_2C_6H_5$ and 3-CN substituted furoxans are reported.

4.4. NO release in A549 cells

NO release in A549 lung adenocarcinoma cancer cells was studied for all furoxan derivatives **1**–**8** in the concentration range 0.1–50 μM, and for **10** in the concentration range 0.1–25 μM. The cells were incubated for 24 h with the abovementioned compounds and then nitrite was detected in the supernatant using the Griess assay. The results are reported in Fig. 1a-b and Figures S3a-b. The NO-release profiles of all the hybrid derivatives were comparable with those of their reference compounds; in the case of compounds **1** and **5**, the release of a small amount of NO was observed only at the highest concentrations (Figure S3a). The same situation was observed with products **2** and **6** (Figure S3b). By contrast, models **3** and **7**, which bear the strongly electron-withdrawing –CN group at the 3-position of the furoxan scaffold, showed a high amount of NO release (Fig. 1a). The NO-releasing capability of **4**, **8** and **10** was lower than that of **3** and **7**, despite the -$C_6H_5SO_2$ group being endowed with electron-withdrawing properties comparable to those of the –CN group (Fig. 1b).

4.5. Cytotoxicity

Cytotoxicity was assessed by measuring the release of lactate dehydrogenase (LDH) to evaluate cell necrosis in A549 cells, incubated for 24 h with the compounds in the 0.1–50 μM concentration range (Figures S4a-d and Fig. 2a-b). In cells, the thiol cofactors responsible for NO release are both free thiols and the cysteinyl residues of proteins. In the former, there is a depletion of the free cellular thiols, resulting in increased oxidative stress, whereas in the latter, protein function is altered (Figures S1 and S2). Thus, the cellular toxicity of the products may be due to both their ability to covalently bind thiol biomolecules and their NO-release.

Rhodamine derivative **9**, which was taken as a reference for an evaluation of the toxicity of the simple rhodamine ring (Figures S4a), showed very low toxicity over the whole range of concentrations tested. The furoxans **5** and **6**, substituted with $–CH_3$ and $–CONH_2$, respectively, did not trigger any significant anticancer activity (Figures S4b-c). Their respective mitochondrial-targeting hybrids **1** and **2** only showed slightly higher cytotoxicity (see Figures S4b-c). This behaviour is in keeping with their poor reactivity with biomolecules and, consequenty, the inefficient NO release of all the products.

By contrast, while the cyano furoxan derivative **7** showed significant cytotoxic activity only at the highest concentration (50 μM), its rhodamine analogue **3** was markedly more active, from 10 μM concentration (Fig. 2a). As the NO-donation capacity of the two cyano derivatives was comparable, we hypothesised that the difference in toxicity can be explained by the potential mitochondrial accumulation of compound **3**.

The 3-phenylsulfonylfuroxan **8** triggered high cellular toxicity from 10 μM concentration, as shown in Fig. 2b, whereas its rhodamine analogue **4**, which possesses similar NO-releasing capacity, caused remarkable cytotoxicity already at 1 μM. This behaviour may be reasonably attributed to its capability of accumulating in mitochondria. Although the NO-releasing ability of two 3-phenylsulfonyl products, **4** and **8**, is certainly lower than that of the related cyano derivatives **3** and **7**, the formers were found to be much more cytotoxic than the latter. Hence, we may infer that the activity of **4** and **8** is mainly due to the covalent labelling of thiol biomolecules via the nucleophilic displacement of the phenylsulfonyl group during diffusion within the cell, and, in particular, after accumulation within the mitochondria.

The cytotoxicity of the hybrid with lysosomal targeting **10** and of the phenothiazine derivative **11** was assessed. Compound **11**, which was used to evaluate the toxicity of the phenothiazine scaffold, showed very low toxicity only at 25 μM (Figure S4d, see SI). Compound **10** and its reference **8**, which displayed similar NO donor ability in cells due to the presence of the 3-phenylsulfonylfuroxan moiety (Fig. 1b), did not exhibit any significant activity in the 0.1–2.5 μM concentration range, while good activity was observed at 10 and 25 μM (Fig. 2c). As the cytotoxicity of compounds **8** and **10** was comparable (Fig. 2c), we can speculate that the accumulation of the 3-phenylsulfonylfuroxan substructure in the lysosomes did not lead to any anticancer-activity benefits. A possible reason for this could be the acidic lysosomal environment, which strongly limits the nucleophilicity of thiol cofactors, and therefore the capacity of the product to release NO and to

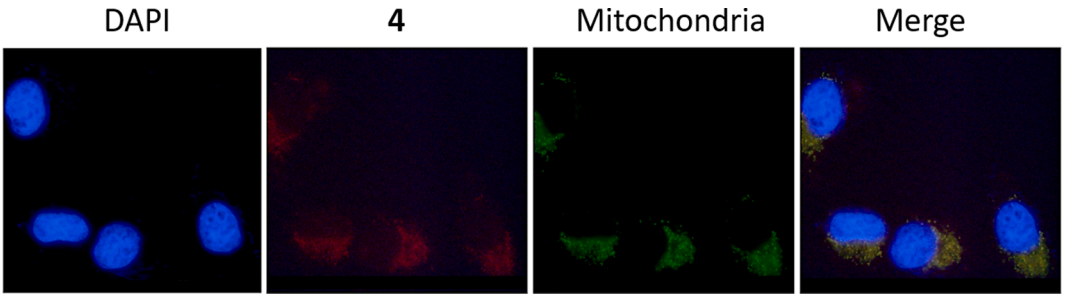

Fig. 3. Fluorescence microscopy images of A549 cells incubated for 24 h with the GFP-E1α pyruvate dehydrogenase expression vector to label mitochondria (green) and then treated with compound **4** (red). Nuclei were counterstained with DAPI. The merged image is shown in the right panel. Scale bars: 10 μm. Micrographs are representative of three experiments with similar results. (For interpretation of the references to colour in this figure legend, the reader is referred to the web version of this article.)

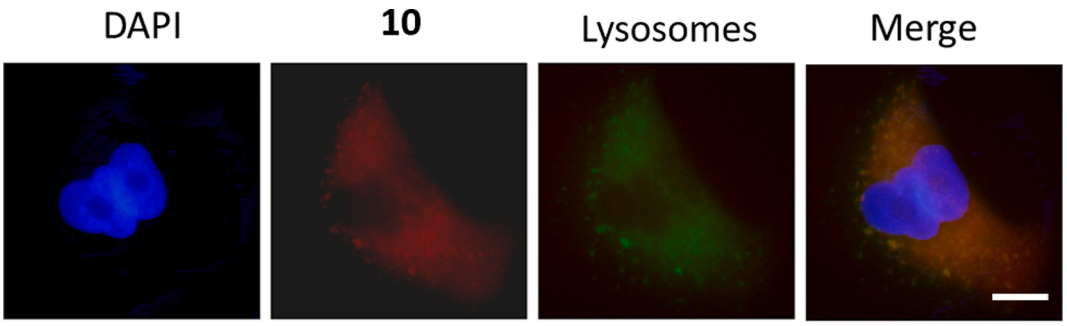

Fig. 4. Fluorescence microscopy images of A549 cells incubated for 24 h with the GFP-Lamp1 expression vector to label lysosomes (green), and then treated with compound **10** (red). Nuclei were counterstained with DAPI. The merged image is shown in the right panel. Scale bars: 10 μm. Micrographs are representative of three experiments with similar results.

covalently bind, and inhibit, proteins. The limited NO-releasing capability of compound **10** in an acidic buffer solution was confirmed (data not shown).

4.6. Intracellular localisation studies in A549 lung adenocarcinoma cancer cells

To demonstrate that intracellular localisation occurred, we carried out a confocal analysis of 3-phenylsulfonylfuroxan derivatives **4** and **10**, used as prototypes of compounds bearing a cellular-organelle targeting moiety. The remarkable fluorescence of the rhodamine moiety is a powerful tool for studying the intracellular localisation of its derivatives. Cells were treated with compound **4** after 24 h of incubation with the GFP-E1α pyruvate dehydrogenase expression vector, which is used to label mitochondria. As expected, compound **4** was identified in mitochondria (Fig. 3) in the fluorescence analysis. The percentage of mitochondria accumulating compound **4** over the total number of mitochondria was 57 ± 6%, suggesting a good mitochondrial targeting. By exploiting the fluorescence of the rhodamine moiety, we also evaluated the accumulation of the cyano derivative **3** via confocal microscopy. This rhodamine derivative was also confirmed to be able to selectively accumulate in mitochondria, as shown in Figure S5.

The fluorescence of the phenothiazine scaffold revealed the accumulation of compound **10** within lysosomes, as shown in Fig. 4. The percentage of lysosomes accumulating compound **10** over the total number of lysosomes was 39 ± 5%, indicating that the vectorisation toward lysosome – although less efficient than the vectorisation toward the mitochondria – was anyway achieved.

5. Conclusions

A study of a set of 3-R-substituted furoxan derivatives and their conjugates with the mitochondrial probe rhodamine B has been performed. The 3-CN and 3-$C_6H_5SO_2$ substituted products showed efficient NO-donation capabilities both in physiological solution and in A549 lung adenocarcinoma cancer cells. These products displayed interesting cytotoxic activity when tested in the abovementioned cells in an LDH assay. In detail, the mitochondria-targeting molecules were clearly more active than their related reference compounds, thus demonstrating the benefits that mitochondrial accumulation has on their activity. Their cellular toxicity may be due to both NO release and the covalent inhibition of thiol biomolecules. The rhodamine hybrid **4**, which contains the 3-$C_6H_5SO_2$-substituted furoxan moiety, was observed to be the most promising member of the series. It triggered high activity across the whole tested concentration range (1–50 μM). A comparative analysis between its toxicity and that of the related 3-CN derivative suggested that its capacity to covalently bind cellular thiols via the nucleophilic displacement of the phenylsulfonyl group plays a paramount role in its cytotoxic properties. An attempt to improve the activity of the 3-phenylsulfonylfuroxan toxophore by accumulating it in lysosomes via conjugation with a phenothiazine scaffold was performed. However, its rhodamine analogue showed higher effectiveness, confirming that mitochondrial targeting remains the best choice for these furoxan substructures.

Declaration of Competing Interest

The authors declare that they have no known competing financial interests or personal relationships that could have appeared to influence the work reported in this paper.

Acknowledgments

This work was supported by Ricerca Locale from the University of Turin. We would like to thank dr. Joanna Kopecka and Costanzo Costamagna for the technical assistance.

Appendix A. Supplementary data

Supplementary data to this article can be found online at https://doi.org/10.1016/j.bioorg.2021.104911.

References

[1] A. Gasco, A.J. Boulton, Furoxans and benzofuroxans, Adv. Heterocycl. Chem. 29 (1982) 251–340.

[2] J. Backes, K. Ebel, W. Friedrichsen, N. Hanold, B. Heinz, A. Hetzheim, U. Kraatz, G. Kirsch, H. Meier, G. Ried, Furazan-2-oxide (Furoxans), in: E. Schaumann (Ed.), Methoden der organischen Chemie (Houben-Weil), Thieme Verlagsgruppe, Stuttgart, New York, Delhi, Rio, 1994, pp. 716–768.

[3] Paton, R.M. 1,2,5-Oxadiazoles., in: Katritzky, A.R., Rees, C.W., Scriven, E.F.V., Compr. Heterocycl. Chem. II, Pergamon Press, New York, 1995, Vol 4, pp.229-265.

[4] A.B. Sheremetev, N.N. Makhova, W. Friedrichsen, Monocyclic furazans and furoxans, Adv. Heterocycl. Chem. 78 (2001) 65–188.

[5] a) M. Feelisch, K. Scheonafinger, E. Noack, Thiol-mediated generation of nitric oxide accounts for the vasodilator actions of furoxans, Biochem. Pharmacol. 44 (1992) 1149–1157;
b) D. Ghigo, R. Heller, R. Calvino, P. Alessio, R. Fruttero, A. Gasco, A. Bosia, G. P. Pescarmona, Biochem. Pharmacol. 6 (1992) 1281–1288;
c) R. Calvino, R. Fruttero, D. Ghigo, A. Bosia, G.P. Pescarmona, A. Gasco, 4-Methyl-3-(arylsulfonyl)furoxans: a new class of potent inhibitors of platelet aggregation, J. Med. Chem. 35 (1992) 3296–3300.

[6] a) C. Medana, G. Ermondi, R. Fruttero, A. Di Stilo, C. Ferretti, A. Gasco, Furoxans as nitric oxide donors. 4-phenyl-3-furoxancarbonitrile: thiol- mediated nitric oxide release and biological evaluation, J. Med. Chem. 37 (1994) 4412–4416;
b) G. Rai, A.A. Sayed, W.A. Lea, H.F. Luecke, H. Chakrapani, S. Prast-Nielsen, A. Jadhav, W. Leister, M. Shen, J. Inglese, C.P. Austin, L. Keefer, E.S. Arner, A. Simeonov, D.J. Maloney, D.L. Williams, C.J. Thomas, Structure mechanism insights and the role of nitric oxide donation guide the development of oxadiazole-2-oxides as therapeutic agents against schistosomiasis, J. Med. Chem. 52 (2009) 6474–6483.

[7] A. Gasco, K. Schoenafinger, The NO-releasing heterocycles, in: P.G. Wang, T.B. Cai, N. Taniguchi (Eds.), Nitric Oxide Donors, WILEY-VCH VerlagGmbH & Co, KGaA Weinheim, 2005, pp. 131–175.

[8] H. Cerecetto, W. Porcal, Pharmacological properties of furoxans and benzofuroxans: recent developments, Mini Rev. Med. Chem. 5 (2005) 57–71.

[9] A. Gasco, R. Fruttero, B. Rolando, Focus on recent approaches for the development of new NO-donors, Mini Rev. Med. Chem. 5 (2005) 217–229.

[10] R.A.M. Serafim, M.C. Primi, G.H.G. Trossini, E.I. Ferreira, Nitric oxide: state of the art in drug design, Curr. Med. Chem. 19 (2012) 386–405.

[11] M. Amir, A.M. Waseem, T. Sana, K. Somakala, Furoxan derivatives as nitric oxide donors and their therapeutic potential, Int. Res. J. Pharm. 6 (2015) 585–599.

[12] E.A. Chugunova, A.R. Burilov, Novel structural hybrids on the base of benzofuroxans and furoxans, Mini-Review. Curr. Top. Med. Chem. 17 (2017) 986–1005.

[13] R. Sharma, J. Joubert, S.F. Malan, Recent development in drug design of NO-donor hybrid compounds, Mini Rev. Med. Chem. 18 (2018) 1175–1198.

[14] Z. Huang, J. Fu, Y. Zhang, Nitric-oxide donor-based cancer therapy: advances and prospects, J. Med. Chem. 60 (2017) 7617–7635. See sections 2.3.2 and 2.3.3 and references therein reported.

[15] a) Y. Guo, Y. Wang, H. Li, K. Wang, Q. Wan, J. Li, Y. Zhou, Y. Chen, Novel nitric oxide donors of phenylsulfonylfuroxan and 3-benzyl coumarin derivatives as potent antitumor agents, ACS Med. Chem. Lett. 9 (2018) 502–506;
b) M. Ingold, L. Colella, P. Hernandez, C. Batthyany, D. Tejedor, A. Puerta, F. Garcia-Tellado, J.M. Padrjn, W. Porcal, G.V. Ljpez, A Focused Library of NO-Donor Compounds with Potent Antiproliferative Activity Based on Green Multicomponent Reactions, ChemMedChem 14 (2019) 1669–1683;
c) Q. Wan, Y. Deng, Y. Huang, Z. Yu, C. Wang, K. Wang, J. Dong, Y. Chen, Synthesis and antitumor evaluation of novel hybrids of phenylsulfonylfuroxan and estradiol derivatives, ChemistryOpen 9 (2020) 176–182;
d) H. Li, K. Wang, Q. Wan, Y. Chen, Design, synthesis and anti-tumor evaluation of novel steroidal glycoconjugate with furoxan derivatives, Steroids 141 (2019) 81–95.

[16] N.M. Sakhrani, H. Padh, Organelle targeting: third level of drug targeting, Drug. Des. Dev. Ther. 7 (2013) 585–599.

[17] C. Riganti, B. Rolando, J. Kopecka, I. Campia, K. Chegaev, L. Lazzarato, A. Federico, R. Fruttero, D. Ghigo, Mitochondrial-targeting nitrooxy-doxorubicin: a new approach to overcome drug resistance, Mol Pharm. 10 (2013) 161–174.

[18] E. Gazzano, L. Lazzarato, B. Rolando, J. Kopecka, S. Guglielmo, C. Costamagna, K. Chegaev, C. Riganti, Mitochondrial Delivery of Phenol Substructure Triggers Mitochondrial Depolarization and Apoptosis of Cancer Cells, Front Pharmacol. 9 (2018) 580.

[19] B. Zhitomirsky, H. Farber, Y.G. Assaraf, LysoTracker and MitoTracker Red are transport substrates of P-glycoprotein: implications for anticancer drug design evading multidrug resistance, J Cell Mol Med. 22 (2018) 2131–2141.

[20] M. Stark, T.F.D. Silva, G. Levin, M. Machuqueiro, Y.G. Assaraf, The Lysosomotropic Activity of Hydrophobic Weak Base Drugs is Mediated via Their Intercalation into the Lysosomal Membrane, Cells. 9 (2020) 1082.

[21] S. Fulda, L. Galluzzi, G. Kroemer, Targeting mitochondria for cancer therapy, Nat. Rev. 9 (2010) 447–463.

[22] D. When, P. Zhu, P. Huang, Targeting cancer cell mitochondria as a therapeutic approach, Future Med. Chem. 5 (2013) 53–67.

[23] Zielonka, J., Joseph, J., Sikora, A., Hardy, M., Ouari, O., Vasquez-Vivar,J., Cheng, G., Lopez, M., Kalyanaraman, B. Mitochondria-targeted triphenylphosphonium compounds: Synthesis, mechanisms of action, and therapeutic and diagnostic applications. Chem. Rev. 117 (2017) 10043-10120, and references therein reported.

[24] Sodano, F., Rolando, B., Spyrakis, F., Failla, M., Lazzarato., L., Gazzano, E., Riganti, C., Fruttero, R., Gasco, A., Sortino, S. Tuning the hydrophobicity of a mitochondria-targeted NO photodonor. ChemMedChem 13 (2018) 1238-1245.

[25] F. Sodano, E. Gazzano, A. Fraix, B. Rolando, L. Lazzarato, M. Russo, M. Blangetti, C. Riganti, R. Fruttero, A. Gasco, S. Sortino, A Molecular Hybrid for Mitochondria-Targeted NO Photodelivery, ChemMedChem 13 (2018) 87–96.

[26] N. Kavčič, K. Pegan, B. Turk, Lysosomes in programmed cell death pathways: from initiators to amplifiers, Biol. Chem. 398 (2017) 289–301.

[27] B. Zhitomirsky, G. Assaraf, Lysosomes as mediators of drag resistance in cancer, Drug Resist. Updat. 24 (2016) 23–33.

[28] R. Halaby, Role of lysosomes in cancer therapy, Res. Rep. in Biol. 6 (2015) 147–155.

[29] N. Fehrenbacher, M. Jäättelä, Lysosomes as targets for cancer therapy, Cancer Res. 65 (2005) 2993–2995.

[30] S. Piao, R.K. Amaravadi, Targeting the lysosome in cancer, Ann. NY Acad. Sci. 1371 (2016) 45–54.

[31] D.A. Wink, J.B. Mitchell, Chemical biology of nitric oxide: insights into regulatory, cytotoxic, and cytoprotective mechanism of nitric oxide, Free Radical Bio. Med. 25 (1998) 434–456.

[32] L.A. Ridnour, D.D. Thomas, S. Donzelli, M.G. Espey, D.D. Roberts, D.A. Wink, J. S. Isenberg, The biphasic nature of nitric oxide responses in tumor biology, Antioxid. Redox Signal. 8 (2006) 1329–1337.

[33] G.C. Brown, Nitric oxide and mitochondria, Front. Biosci. 12 (2007) 1024–1033.

[34] Li,Y., Wu, W., Yang, J., Yuan, L., Liu, C., Zheng, J., Yang, R. Engineering a nanolab for the determination of lysosomal nitric oxide by the rational design of a pH-activatable fluorescent probe. Chem. Sci. 7 (2016) 1920-1925, and references therein reported.

[35] M. Li, J.X. Xia, R. Tian, J. Wang, J. Fan, J. Du, S. Long, X. Song, J.W. Foley, X. Peng, Near-infrared light-initiated molecular superoxide radical generator: rejuvenating photodynamic therapy against hypoxic tumors, J. Am. Chem. Soc. 140 (2018) 14851–14859.

[36] A. Di Stilo, S. Visentin, C. Cena, A. Marcello, G.E. Gasco, A. Gasco, New 1,4-Dihydropyridines Conjugated to Furoxanyl Moieties, Endowed with Both Nitric Oxide-like and Calcium Channel Antagonist Vasodilator Activities, J. Med. Chem. 27 (1998) 5393–5401.

[37] K. Chegaev, L. Lazzarato, B. Rolando, E. Marini, G.V. Lopez, M. Bertinaria, A. Di Stilo, R. Fruttero, A. Gasco, Amphiphilic NO-donor antioxidants, ChemMedChem 2 (2007) 234–240.

[38] M. Bertinaria, S. Guglielmo, B. Rolando, M. Giorgis, C. Aragno, R. Fruttero, A. Gasco, S. Parapini, D. Taramelli, Y.C. Martinsc, L.J.M. Carvalhoc, Amodiaquine analogues containing NO-donor substructures: Synthesis and their preliminary evaluation as potential tools in the treatment of cerebral malaria, Eur J Med Chem 46 (2011) 1757–1767.

[39] S. Verma, U.W. Sallum, H. Athar, L. Rosenblum, J.W. Foley, T. Hasan, Antimicrobial Photodynamic Efficacy of Side-chain Functionalized Benzo[a] phenothiazinium Dyes, Photochem. 85 (2009) 111–118.

[40] E. Aldieri, F. Fenoglio, F. Cesano, E. Gazzano, A. Gulino, D. Scarano, G. Attanasio, G. Mazzucco, D. Ghigo, B. Fubini, J. Toxicol. Environ. Health A. 76 (2013) 1056–1071.

[41] C. Riganti, E. Miraglia, D. Viarisio, C. Costamagna, G. Pescarmona, D. Ghigo, A. Bosia, Nitric oxide reverts the resistance to doxorubicin in human colon cancer cells by inhibiting the drug efflux, Cancer Res. 65 (2005) 516–525.

[42] Testa, B., Van de Waterbeemd, W., Folkers, G., Guy, R. Pharmacokinetic Optimization in Drug Research. Verlag Helvetica Chimica Acta, WILEY-VCH. 2001, Part IV, 275-304.

[43] C. Hansch, A. Leo, Exploring QSAR, Fundamentals and applications in chemistry and biology. American Chemical Society, Washington, 1995.

[44] a) R. Fruttero, G. Sorba, G. Ermondi, M. Lolli, A. Gasco, Structural investigations in benzenesulfonylfuroxan derivatives and related compounds, Il Farmaco 52 (1997) 405–410;
b) G. Sorba, C. Medana, R. Fruttero, C. Cena, A. Di Stilo, U. Galli, A. Gasco, Water soluble furoxan derivative as NO prodrugs, J Med. Chem. 40 (1997) 463–469.